Supplementary Information (SI) for Journal of Materials Chemistry A.

Bio-based Adaptable Dynamically Cross-linked Networks and Their Composites: Multiple Stimulus Response and Potential Electromagnetic Shielding Applications

Yun Hu[a], Ye Sha[b], Lei Chen[c], Yufeng Ma[c], Qin Huang[d], Meng, Zhang[a], Puyou Jia[a*], Yonghong Zhou[a]

[a] Institute of Chemical Industry of Forest Products, Chinese Academy of Forestry (CAF), Jiangsu Co-Innovation Center of Efficient Processing and Utilization of Forest Resources, Jiangsu Province, 16 Suojin North Road, Nanjing 210042, China.

[b]College of Science, Nanjing Forestry University, 159 Longpan Road, Nanjing, 210037, China.

[c] College of Materials Science and Engineering, Nanjing Forestry University, 159 Longpan Road, Nanjing 210037, China.

[d] Key Laboratory of Chemistry and Engineering of Forest Products, State Ethnic Affairs Commission, Guangxi Key Laboratory of Chemistry and Engineering of Forest Products, Guangxi Minzu University, Nanning 530006, China

(*Corresponding Authors: E-mail: jiapuyou@icifp.cn (P. J.)).

Characterization

Fourier transform infrared spectrometry (FT-IR) spectra were taken on a PerkinElmer spectrum 100 FTIR spectrometer. 300 MHz ^{1}H NMR spectra were recorded on a Bruker Avance III HD 300 spectrometer using $CDCl_3$ as the solvent with tetramethylsilane (TMS) as an internal reference. The gel content was determined by extraction method. A resin of approximately 0.5 g was first accurately weighed (recorded as m_0), then extracted with acetone for 24 h, and dried in a vacuum oven at 50 ^{o}C for 24 h, and weighed again (recorded as m_1). The value was calculated by formula (m_1/m_0)*100%. The rheological properties were measured using an oscillatory rheometer (Anton Paar, MCR92) using a parallel plate–plate geometry with a size of 50 mm diameter circular disc. Thermogravimetric analysis (TGA) was carried out on a Q5000 TGA system (TA Instruments), ramping from 40 to 600 °C at a heating rate of 10 °C min^{-1} under a nitrogen flow at 25 mL min^{-1}. Glass transition temperature (T_g) was recorded through differential scanning calorimetry (DSC) conducted on a DSC 2000 instrument (TA Instruments).Crosslinking density of polymers were tested with dynamic mechanical analysis (DMA) using a Q800 DMA (TA Instruments, New Castle, DE) with a frequency of 1 Hz in a stretching mode under N_2 atmosphere. The temperature ranged from -80 to 140 °C at a heating rate of 3 °C /min with the size of 80 ×6 × 1 mm^3. The shape memory behaviors of the sample was tested by DMA analysis. The rectangular sample (30 × 6 × 1 mm^3) was heated to 110 °C, then 0.1 MPa external pressure was applied and cooled to 25 °C with a cooling rate of 5 °C/min to completely remove the external stress. Then the temperature was heated to 110 °C at the speed of 5 °C/min, and the shape of the sample was restored. This process was repeated four times. The following formula was used to calculate the shape fixation rate (R_f) and shape recovery rate (R_r).

$$R_f = \frac{\varepsilon_d}{\varepsilon_{load}} \times 100\%$$

where ε_{load}, ε_d, and ε_{rec} represent the fixed strain of each cycle, initial strain upon loading, and recovered strain, respectively. Tensile tests were taken on an E43.104 Universal Testing Machine (MTS Instrument Crop., China). Dog-bone shaped samples with a length of 20 mm and a width of 5.0 mm were tested at room temperature with a crosshead speed of 20 mm/min. Five replicate samples were used to obtain an average value for each sample. The water contact angle was measured using a contact angle meter(SL2008 solon contact angle meter, China) with a 3 μL water droplet. The average value of five specimens and deviation were calculated. Optical microscopy was obtained from a Leica metallographic microscope (Germany) to calculate the self-healing efficiency. Solvent resistance was investigated by immersing the samples in deionized water, ethanol, tetrahydrofuran, ethyl acetate, 20 wt% sulfuric acid solution, 1 M NaOH solution, petroleum ether, and dimethyl formamide (DMF) for 48h h at 25 °C. FLIR thermal imager 3rd generation FLIR one Pro mobile phone external probe infrared thermal imager one pro (Android version -20 ~ 400 °C). The electrical performance uses Unilever UTP3315TFL DC regulated power supply (0-32 V, Korea). The EMI SE performance of composites was measured using a Agilent PNA-N5244A vector network analyzer within 8.2–12.4 GHz in X band. The corresponding dimension of samples was 20 ×10×1 mm^3. The dielectric constant was measured using a Agilent 4294A dielectric spectrometer, with a film thickness of 1.0 mm, and a testing frequency of 50Hz-1MHz. The morphology of the materials were tested by scanning electron microscopy (SEM) using a Zeiss supra55.

Chemical structure of of TO, ET, MET composition and PNMET0.

Tung oil (TO), ethanolamides of tung oil fatty chains (ET), tung oil-based UV-curable prepolymer(MET composition), and PNMET0, PNMET1~3 were synthesized (Fig. S1a and b) and characterized by FT-IR and ^1H NMR (Fig. S2 a & b). In the FT-IR spectrum of ET, a peak at 3315 and 1662 cm^{-1} corresponding to the OH/NH and carbonyl group appeared, and the peak at 1745 cm^{-1} attributing to the ester bond of triglyceride of tung oil cannot be observed [1]. In the FT-IR of MET, the peak at 3315 cm^{-1} showed stronger compared with ET, and the peaks at 1742 and 852 cm^{-1} were attributed to the formation of the ester bond and double bond of methacrylic acid after esterfication, respectively. In the FT-IR of PNMET0, the disappearance of double bonds of methacrylic acid and conjugated double bond at 852, 3020 and 1012 cm^{-1} indicated that active double bonds participated in the reaction under UV conditions and PNMET0 was successfully fabricated. In the ^1H NMR spectrum of TO, the signals at 4.2 and 5.3 ppm were assigned to protons of methylene from triglycerides [2]. The absorption peak at 3.3 ppm in the ^1H NMR spectrum of ET was assigned to protons of OH/NH. In the ^1H NMR of MET, the new absorption peaks at 11.0 and

12.0 ppm were assigned to protons of double bond from methacrylic acid, and the peak at 9.0 ppm was attributed to the protons on the carboxyl of methacrylic acid. Combining these results of FT-IR and ^{1}H NMR, it can be confirmed the successful preparation of MET composition and PNMET0.

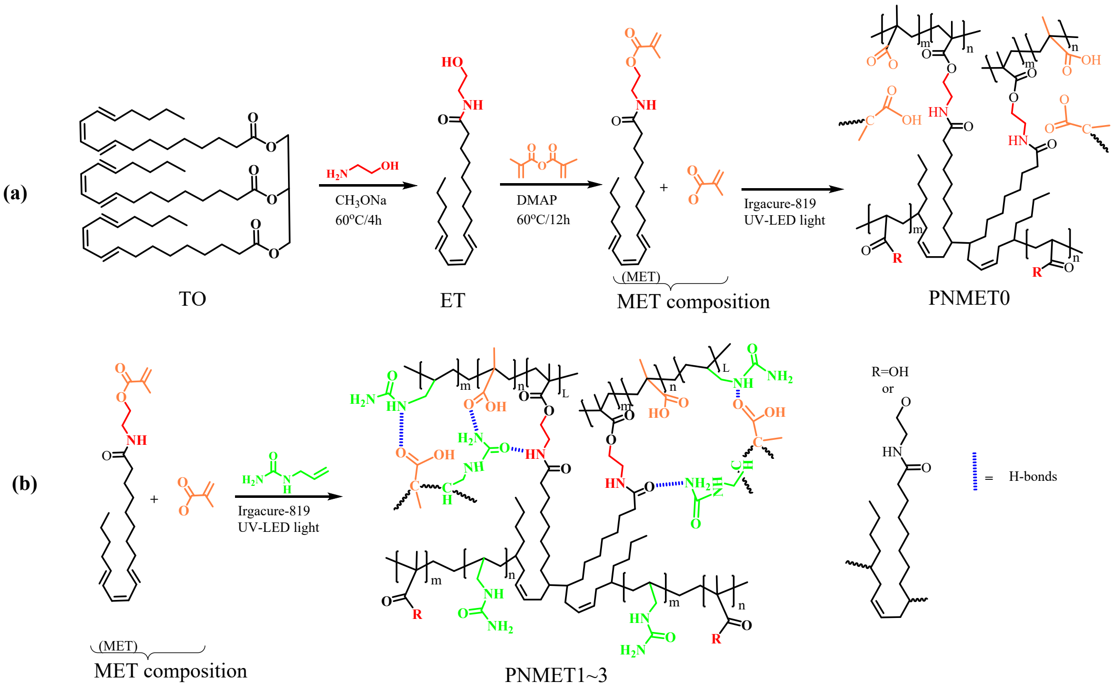

Fig. S1 (a) Synthetic route of PNMET0. (2) Synthetic route of PNMET1~3.

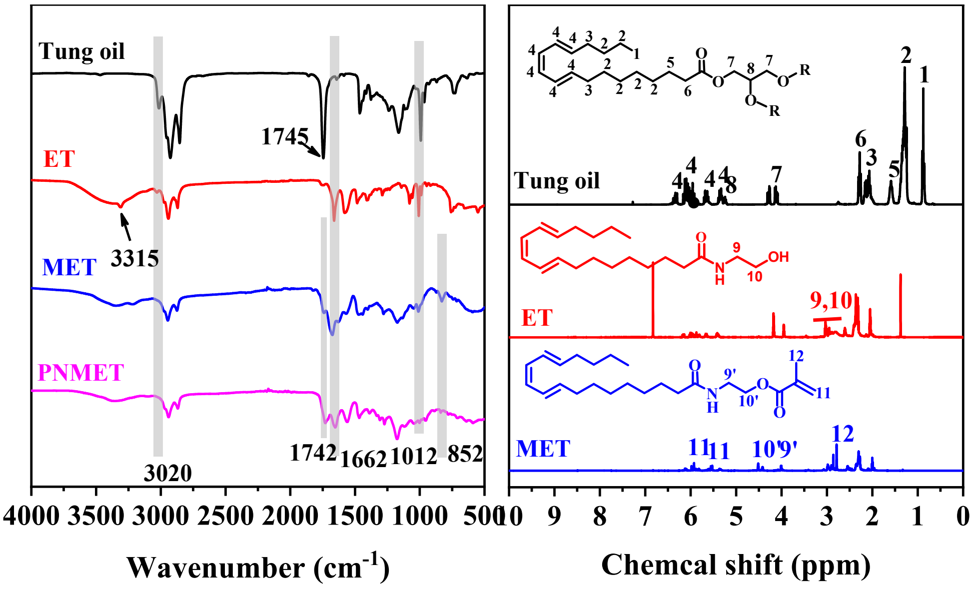

Fig. S2 (a) FT-IR spectra of TO, ET, MET, and PNMET0. (b) ^{1}H NMR spectra of TO, ET, and MET.

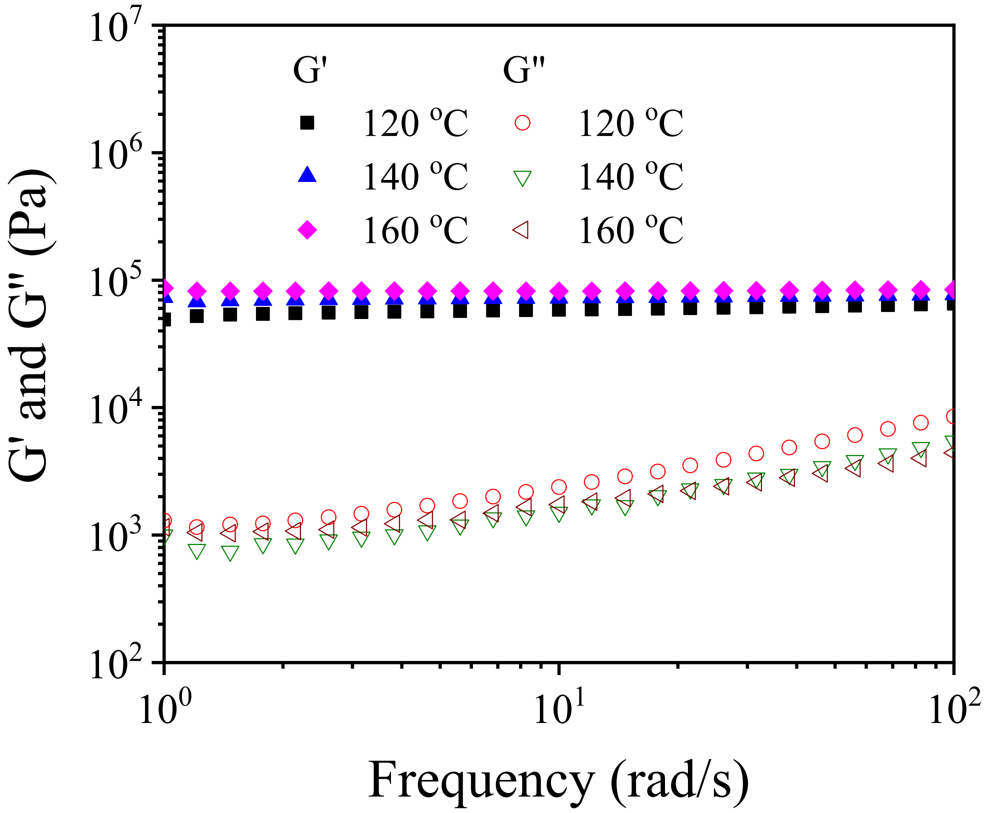

Fig. S3. Rheology frequency sweep of the PNMET1 at elevated temperature.

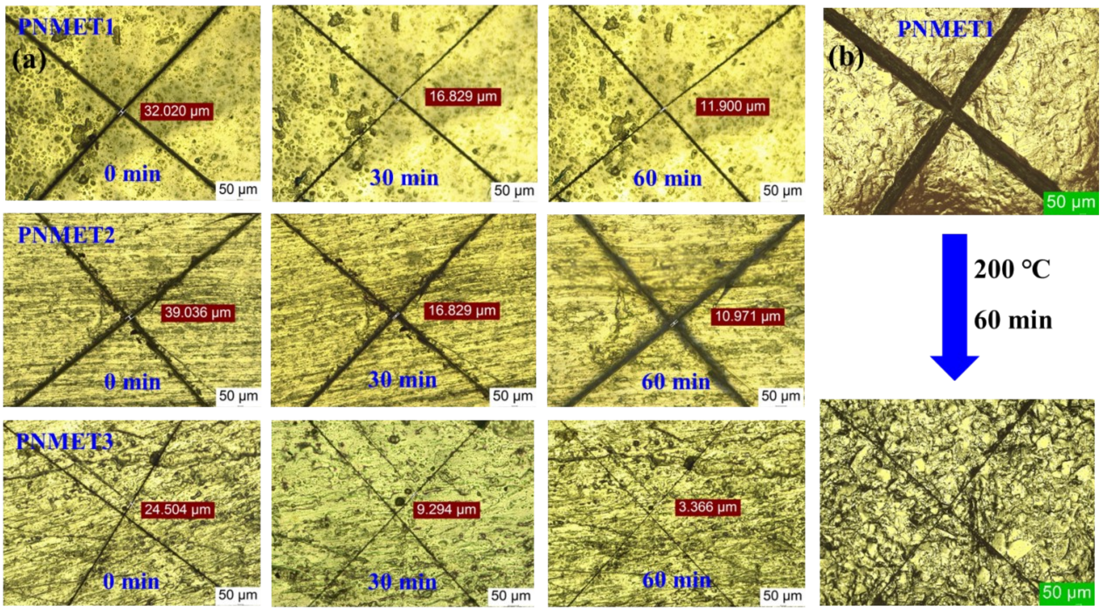

Fig. S4. (a) Self-healing of PNMET1, PNMET2, and PNMET3 at 80 °C for 30 min and 60 min, respectively. (b) Self-healing of PNMET1 at 200 °C for 60 min.

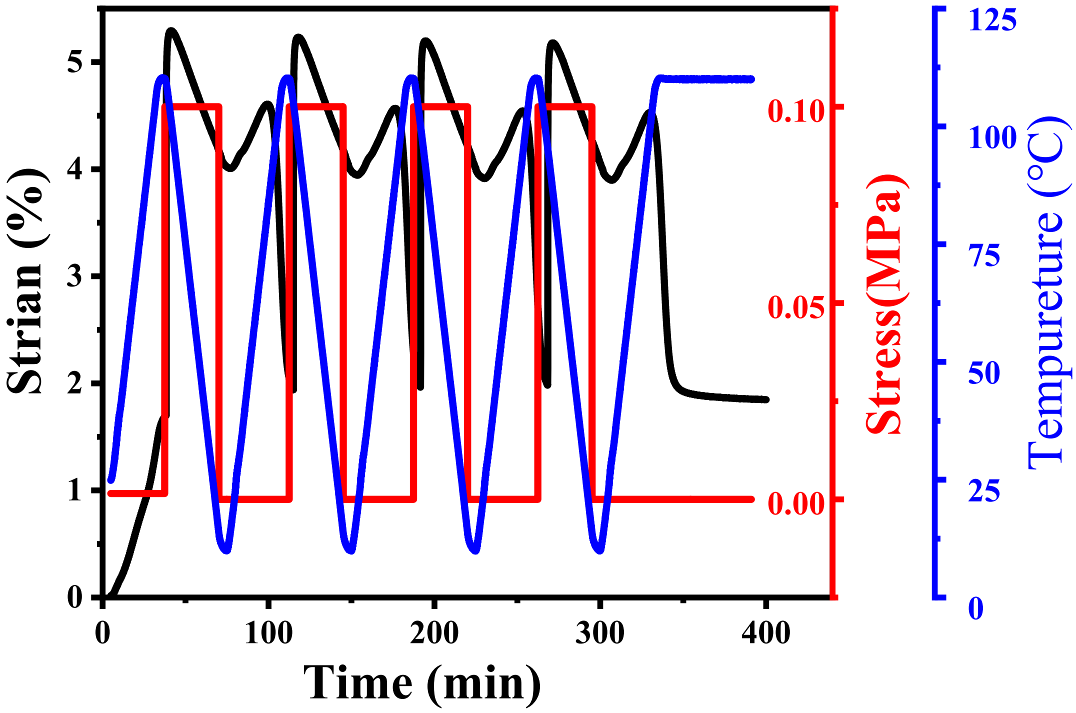

Fig. S5. Shape memory curves of PNMET1 by DMA.

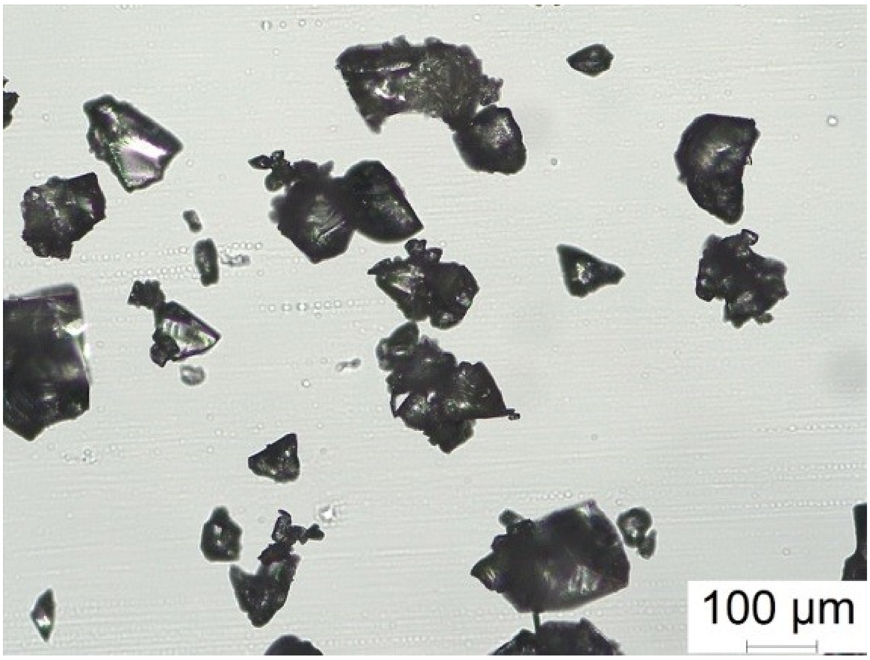

Fig. S6. Microstructure of PNMET1 powder.

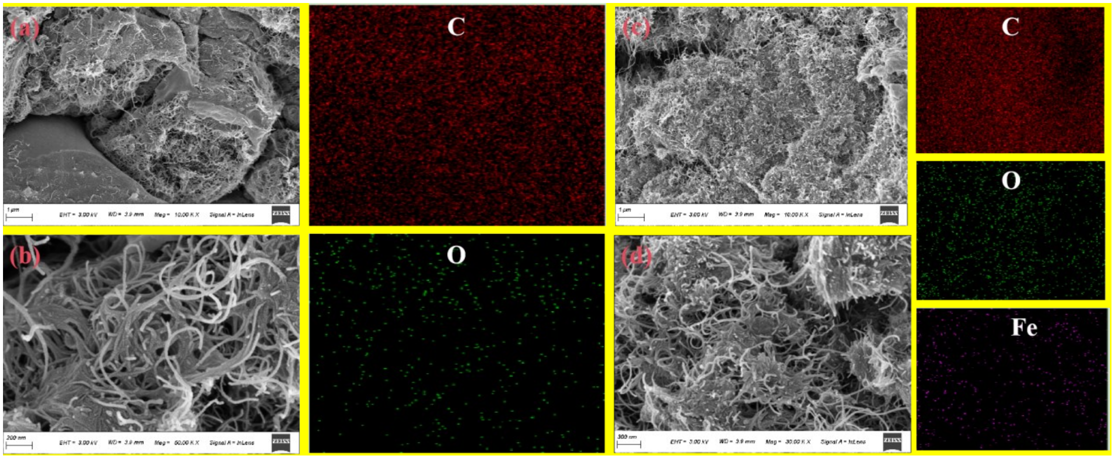

Fig. S7 (a) and (b): SEM and EDS mapping images of PNMET/MWCNT(4wt%) composite. (c) and (d): SEM and EDS mapping images of PNMET/MWCNT(4wt%)@Fe_3O_4 (2wt%) composite.

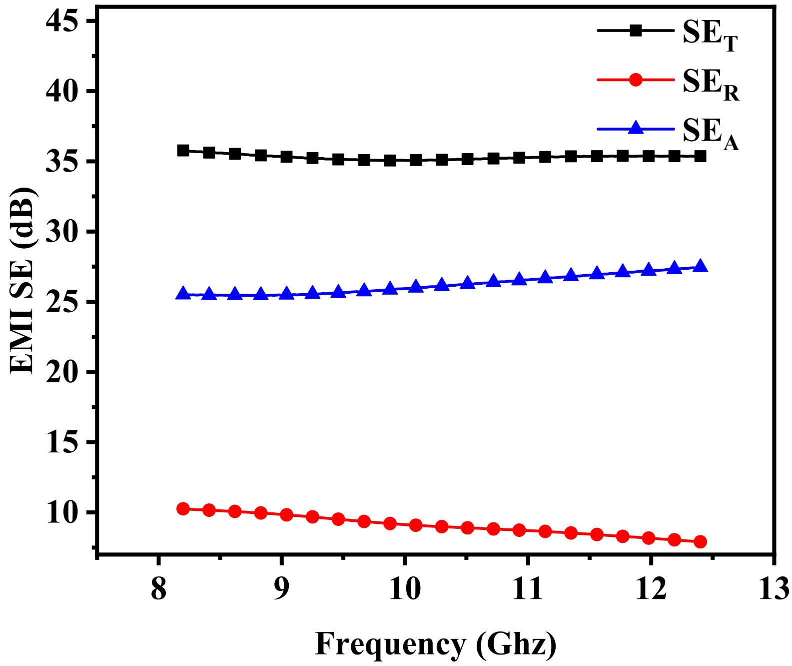

Fig. S8. EMI SE (the total EMI SE (SE_T), reflection EMI SE (SE_R), and absorption EMI SE (SE_A)) of PNMET/ MWCNT (10 wt%) composite in X-band.

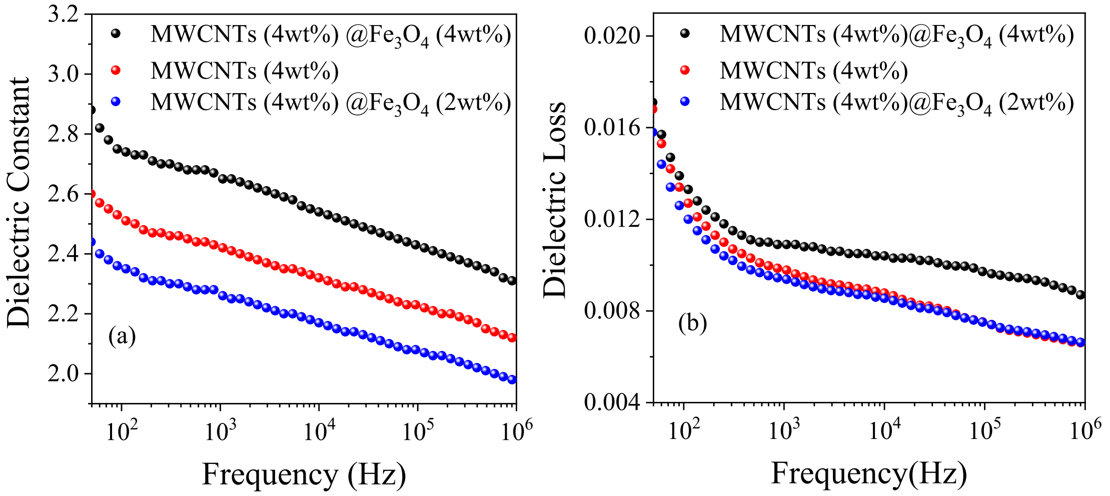

Fig.S9. Frequency dependence of (a) dielectric constant and (b) dielectric loss of PNMET/MWCNT(4wt%)@Fe_3O_4(0-4w%) composite.

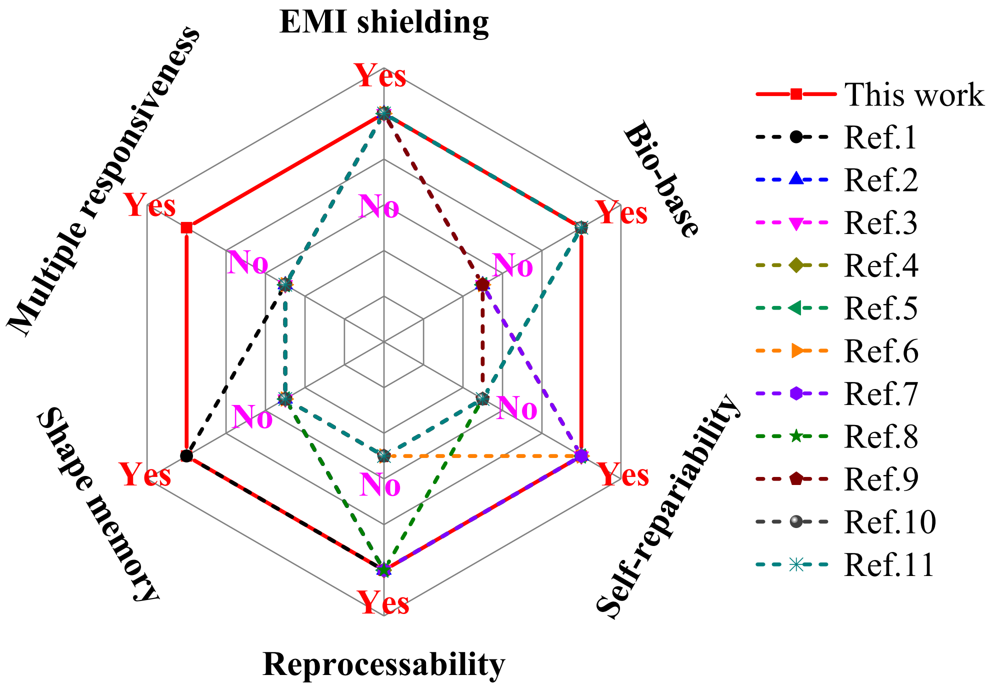

Fig. S10. Parameters for the bio-based dynamically cross-linked networks for electromagnetic interference shielding materials in this work, and reported in the literatures.

Table S1. Formulation and gel content of PNMET0 and PNMET1~3.

Samples	**MET/g**	**N-allylurea/g**	**Irgacue-819/g**	**Gel content/%**
PNMET0	4	0	0.20	75.6 ± 2.3
PNMET1	4	0.25	0.21	85.6 ± 1.5
PNMET2	4	0.50	0.23	83.9 ± 2.7
PNMET3	4	1.00	0.25	80.4 ± 2.2

Table S2 T_5, T_{50}, and R_{600} of PNMET0 and PNMET1~3.

Samples	T_{gDCS}**/ °C**	T_5**/°C**	T_{50}**/°C**	R_{600}**/%**	T_{p}**/°C**
PNMET0	-	223.2	411.9	8.3	447.1
PNMET1	-21.8	204.8	408.1	4.8	441.6
PNMET2	-25.8	186.5	403.7	7.4	439.1
PNMET3	-26.4	175.6	388.7	5.6	438.9

Table S3 Thermal properties of PNMET0 and PNMET1~3.

Samples	E_{25}**/MPa**	T_{g}**/ °C**	$E_{T_{\mathrm{g}}+30}$**/MPa**	v_{e} **/mol·m**$^{-3}$
PNMET0	242.2	58.4	4.1	460.3
PNMET1	638.4	67.8	6.9	751.1
PNMET2	134.3	48.3	3.1	350.3
PNMET3	23.3	28.6	2.7	328.7

Table S4 Mechanical parameters of PNMET0 and PNMET1~3.

Samples	**Tensile strength/MPa**	**Tensile breaking strain/%**	**Toughness (MJ/m^3)**	**Young's modulus (MPa)**
PNMET0	16.4 ± 2.5	12.4 ± 3.1	1.13 ± 0.1	162.7 ± 20.3
PNMET1	13.1 ± 1.8	13.0 ± 2.6	0.92 ± 0.1	120.6 ± 12.1
PNMET2	8.8 ± 1.6	28.9 ± 4.1	2.12 ± 0.7	77.9 ± 8.9
PNMET3	2.3 ± 0.6	68.8 ± 5.9	1.03 ± 0.1	12.4 ± 3.1

Table S5 Swelling properties of PNMET0 and PNMET1~3.

Samples	**Water/%**	**Ethanol/%**	**Acetone/%**	**Toluene /%**
PNMET0	4.87 ± 1.0	3.07 ± 0.6	12.97 ± 2.2	6.38 ± 0.7
PNMET1	2.28 ± 0.5	2.19 ± 0.3	11.58 ± 1.6	5.26 ± 1.2
PNMET2	6.81 ± 1.5	3.19 ± 1.1	13.95 ± 2.4	7.84 ± 0.9
PNMET3	7.64 ± 1.4	4.43 ± 1.6	15.62 ± 2.8	10.8 ± 2.1

Table S6 Mechanical properties of PNMET0 and PNMET1 after recycling.

Samples	**Tensile strength /MPa**	**Recycling Efficiency /%**	**Tensile breaking strain/%**	**Recycling Efficiency /%**
PNMET0	16.42	-	12.41	-
Recycled PNMET0	15.53	94.58	5.26	42.39
PNMET1	13.02	-	13.03	-
Recycled PNMET1	17.74	136.25	8.21	63.01

Table S7 The R_f and R_f of PNMET1.

	PNMET1			
Number of cycles	1	2	3	4
$\boldsymbol{R_f}$**/%**	76.2	73.6	73.8	74.0
$\boldsymbol{R_r}$**/%**	52.5	49.7	49.4	52.3

Table S8 Comparison between this work and recently published composites with EMI Shielding Performance.

Ref.	EMI shielding	Bio-base	Self-repariability	Reprocessability	Shape memory	Multiple responsiveness
[3]	YES	NO	YES	YES	YES	NO
[4]	YES	NO	YES	YES	NO	NO
[5]	YES	NO	YES	YES	NO	NO
[6]	YES	NO	YES	YES	NO	NO
[7]	YES	NO	YES	YES	NO	NO
[8]	YES	NO	YES	NO	NO	NO
[9]	YES	NO	YES	YES	NO	NO
[10]	YES	YES	NO	YES	NO	NO
[11]	YES	NO	NO	NO	NO	NO
[12]	YES	YES	NO	NO	NO	NO
[13]	YES	YES	NO	NO	NO	NO
This work	**YES**	**YES**	**YES**	**YES**	**YES**	**YES**

1. Z Kou, Y Hu, Y Ma, L Yuan,L Hu, Y Zhou, Jia P. *Ind Crop Prod.* 2023, **195**, 116401.

2. F Song, X Zou, L Yuan, Y Sha, Q Zhao, M Zhang, L Hu, X Zhu, P Jia, Y Zhou. *J Mater Chem A*. 2022, **10**, 15766-15775.

3. P Yan, H Yujia, W Qi, Z Yong, H Guangsu, R Qichao, W Jinrong. *Carbon.* 2020,

166, 56-63.

4. T Wang, W Yu, C Zhou, W Sun, Y Zhang, L Jia, J Gao, K Dai, D Yan, Z Li. *CompoPart B-Eng.* 2020, **193**, 108015.

5. H Fang, W Ye, K Yang, K Song, H Wei, Y Ding. *CompoPart B-Eng.* 2021, **215**, 108782.

6. H Mao, J Hu, J Shiu, S Rwei, C Chen. *Polym Test.* 2023, **127**, 108200.

7. Y Bai, B Zhang, G Fei, Z Ma. *Chem Eng J.* 2023, **478**, 147382.

8. L Chen, K Guo, S Zeng, L Xu, C Xing, S Zhang, B Li. *Carbon*. 2020, **162**, 445-454.

9. P Das, A Katheria, J Nayak, S Das, K Nath, S Ghosh, Naskar, N Das. *Colloid Surface A*. 2023, **676**, 132244.

10. C Lee, C Lin, L Wang, Y Lee. *Chem Eng J.* 2023, **468**, 143447.

11. Y Lee, C Cheng, C Chiang, Z Tong, L Wang, C Lee. *J Mater Chem C.* 2021, **9**, 15622-15640.

12 V. Selvaraj, J Subramanian, E Jeyamani, A Azeez, R Keerthivasan. *J Appl Polym Sci.* 2022, **140**, e53386.

13. H Kang, S Luo, H Du, L Han, D Li, L Li, Q Fang. *Polymers*. 2022, **14**, 970.